Data-Driven Study of LV Distribution Grid Behaviour with Increasing Electric Vehicle Penetration

Yu, Yunhe; Reihs, David; Wagh, Saumitra ; Shekhar, Aditya; Stahleder, Daniel ; Chandra Mouli, Gautham Ram; Lehfuss, Felix; Bauer, Pavol

DOI
10.1109/ACCESS.2021.3140162

Publication date
2022

Document Version
Final published version

Published in
IEEE Access

IEEE Access
Multidisciplinary ⋮ Rapid Review ⋮ Open Access Journal

Received December 15, 2021, accepted December 29, 2021, date of publication January 4, 2022,
date of current version January 18, 2022.

Digital Object Identifier 10.1109/ACCESS.2021.3140162

Data-Driven Study of Low Voltage Distribution Grid Behaviour With Increasing Electric Vehicle Penetration

YUNHE YU[1], DAVID REIHS[2], SAUMITRA WAGH[1], ADITYA SHEKHAR[1], (Member, IEEE), DANIEL STAHLEDER[2], GAUTHAM RAM CHANDRA MOULI[1], (Member, IEEE), FELIX LEHFUSS[2], AND PAVOL BAUER[1], (Senior Member, IEEE)

[1]Department of Electrical Sustainable Energy, Delft University of Technology, 2628 CD Delft, The Netherlands
[2]Department of Electric Energy Systems, Austrian Institute of Technology, 1210 Vienna, Austria

Corresponding author: Yunhe Yu (y.yu-4@tudelft.nl)

The work of this paper is part of the project Orchestrating Smart Charging in Mass Deployment (OSCD, https://www.oscd.eu/). The OSCD project is funded by ERA-NET Cofund Electric Mobility Europe (EMEurope).

ABSTRACT In this paper, the impact of Electric Vehicle (EV) uncontrolled charging with four levels of EV penetration in overall 21 real low voltage distribution grids in two seasons are analysed. The employed real grid data is provided by distribution system operators from three European countries: Austria, Germany and the Netherlands. At least six grids in each country were considered and they are categorised into three types, namely rural grids, suburban grids and urban grids. The EV charging data used in this study is based on real measurements or surveys. The seasonal and the weekday-weekend factors are also considered in the EV charging impact research. Three key congestion indicators, the transformer loading, line loading and node voltage as well as several other evaluation indexes are studied. The results reveal that the majority of the simulated grids had no or minor moments of mild overloading while the rest grids had critical issues. Among all the grids, suburban grids are most vulnerable to massive EV integration. Out of the evaluated grids, those who are located in Germany have the highest redundancy for high EV penetration accommodation. Overall, the impact of uncontrolled EV charging depends on the combination of EV charging demand as well as the grid inherent features.

INDEX TERMS Electric vehicle (EV), low voltage distribution grid, uncontrolled charging.

I. INTRODUCTION

It is well established that the market penetration of Electrical Vehicles (EVs) is rapidly growing and consequentially, the technological impact of this mass deployment has attracted considerable research attention [1]–[5]. The grid impact is particularly relevant because the conventional uncontrolled charging strategy, in which the EVs start to draw the rated power at the instant of connection, can result in numerous simultaneous charging events [6]. The widely implemented level 2 AC charging has a rated power that can be high as 22 kW (3 phase 32A) [7]. Such charging requirements due to an anticipated increase in EV penetration levels can stress the facilitating distribution grid infrastructure, such that it can cause transformer overloading and lifetime reduction [2]–[4], [8], [9], line overloading [2], [4], [10], voltage drop below acceptable limits at the far-end of the feeder [2]–[4], [9], higher distribution losses [2]–[4], power mismatch between supply and demand, phase imbalance [4], [9], as well as harmonic distortion [11]. It is suggested in [5] that future work investigating the grid impact with increased EV penetration can be scaled up when real-world transportation and power data becomes available. The specific aim of our paper is to contribute towards this goal and provide a realistic insight based on the acquired on-field data sets.

The associate editor coordinating the review of this manuscript and approving it for publication was Nagesh Prabhu.

A. LITERATURE REVIEW

The influence of data-driven uncertainties in driver behaviour and energy demand of the EVs toward the grid impact of uncontrolled charging is considered in [3], [4], [12], [13]. For example, [3] uses data of the daily miles driven and the

arrival times to show that the load demand for a 34-node IEEE test feeder has no noticeable change from 3:00 a.m to 11:00 a.m even with 45 % EV penetration level, resulting in approximately 11 % (in summer) and 15 % (in winter) increased peak from the average loading ratio. In [4] the IEEE RTS load profile data was clustered into representative curves to show there is no loading variation for IEEE 123-node test feeder substation in 3:00 a.m to 9:00 a.m window even considering 100 % EV penetration, but the probability of overloading the 50 kVA transformer increased to 35 % with the peak demand increasing linearly by 2-3 % for every 10 % increase in EV penetration. Study [12] tested four charging methods with several scenarios including the uncontrolled method with a 33-buses sample grid and assess the impact on the distribution system. It is found that EV penetration levels of 28.1-46.5% can be accommodated in the system without violating the grid constraints. An 11 kV 38-node typical UK sample distribution system was used in [13] to test three representative uncontrolled EV charging scenarios and one ''smart'' charging scenario. The results indicate a 35.8% peak load growth with 20% EV penetration in the worst uncontrolled charging case. However, these papers consider standard test grids in the study and therefore, extending the insight with real distribution grid data can be useful.

Research [14] studies the charging impact of 0 to 500 EVs in a modified IEEE 13-bus system as well as a 25-bus real Taiwan distribution system. One thousand iterative Monte Carlo simulations were conducted to study the stochastic effect of both the feeder load and EV charging while using measured data at two large charging stations. It appears in the results that for the real grid there is no voltage drop violation even with the worst scenario, but for the IEEE standard grid the congestion problems are already present with 200 EVs and the under-voltage problem develops earlier than the line congestion. Two distribution systems located at a residential-urban area and an industrial-residential area with 35, 51, 62% EV penetration levels were modelled in [15]. This study examines the impact of two charging patterns (valley and peak hours) and found that a maximum of 19% total actual network cost is required to increase the capacity and accommodate all charging requests. Paper [16] investigates three real distribution grids (urban, rural and commercial) with 20, 40, 60, 80 % EV penetration levels. The result shows that transformer overloading can already be observed for 20% EV penetration in the urban grid, but in the rural grid, the EV penetration can increase to 40%. None of the grids has under-voltage problems, and line loading is not discussed in the paper. Study [17] investigates EV integration into a cluster of real distribution grids with 39-feeders in the USA. The examined network contains a mix of area types, where half of the feeders supply residential areas and the rest are distributed among industrial, commercial and agricultural areas. The EV charging data is modelled based on real vehicle itineraries and only one EV penetration level (one EV per household) is analysed. The study concludes that 58% of the feeders reach their power capacity limit and 47% of the grids have shown line overloading problem, yet none of the grid's experiences voltage drop to lower than 0.9 p.u.. What is the maximum number of EVs that can be integrated into the grid is explored in [18]; the mobility of EVs are also considered. Two Swedish distribution networks where one residential network with 3 feeders and 26 substations and one commercial network with 4 feeders and 9 substations are employed. When the system runs in normal conditions, only in one case which all EVs only charge at home in the residential area can the grid accommodate less than 100% EV penetration. However, if any feeder is disconnected due to maintenance, the grid can experience overloading even without any EV charging. Besides, none of the grids has any under-voltage problem in the simulations. Study [19] considers an even larger area in the Netherlands where the simulated network contains 55 distribution systems that consist of a total of 12,000 substations. It is assumed in this study that EVs only charge at home with two fixed power levels, and the charging profile is generated based on a big dataset of Dutch driving patterns. An increase EV penetration trend along with time up to 75% in the year 2040 was assumed and 49% of the transformers experience overloading issues at the worst scenario. All the works mentioned above focus on the big scale in which the grid performance of MV distribution systems is evaluated as a whole, a closer insight into each LV distribution grid would be beneficial.

While [20] investigates a real LV distribution grid in Norway to suggest an overload and under-voltage tolerance up to 20% and 50% EV penetration level respectively, the paper highlights the limitation that the charging profile is derived from a single household load profile and thereby neglecting the uncertainties in arrival and departure time as well as energy demand that can occur with mass deployment of EVs. The results suggest a 20% EV penetration tolerance boundary with no grid limitation violation.

In paper [21], historical driving data was used to generate home EV charging profiles and four EV penetration levels from 25% to 100% were tested on a real Danish LV distribution grid model. The paper explores grid loading and phase unbalance caused by EV charging. It is found in this study that the loading induced by EV charging at home is not high as expected due to a relatively low simultaneous factor (45%). It's also concluded that a 30-50% EV penetration is the maximum acceptable uncontrolled charging integration rate, depending on the characteristics of the grid. Researchers of [22], [23] ran a plentiful of Monte Carlo simulations to investigate the EV charging impact of 0-100% penetration levels on two real British LV distribution grids whose grid types are not specified. The EV data implemented for simulation is originally from a one-year-long site trial. The main discovery regarding uncontrolled EV charging impact is: the transformer overloading is the main issue in network 1 while voltage drop is the main challenge of network 2. The upper limit of EV accommodation without grid congestion

problem is 40% for network1 (thermal limit) and 20% for network 2 (voltage limit). Another study inspects both real transmission and distribution grids performance with 0-100% EV penetration with real EV charging data [24]. In the paper, three LV distribution grids were investigated, rural, suburban and urban. It is found that with 100% EV penetration, there is voltage drop violation and possible transformer overloading. However, the results might still vary a lot and strongly depend on the local EV, households and grid features. Besides, it is predicted that by 2030, 10% of the distribution grids will suffer from transformer overloading issues and 5% of the distribution grids will have under-voltage problems. In total, 28% of grids would require upgrades.

B. CONTRIBUTIONS

The focus of this paper is to use measured probabilistic data pertaining to energy demand, arrival and departure time of EVs to investigate the impact of uncontrolled charging for several actual grids in Europe. The findings are useful and add to the body of knowledge in the following aspects:

- We show that Suburban grids have relatively higher congestion issues compared to rural and urban grids.
- We also investigate how the type of grid in different countries affects the grid impact of uncontrolled EV charging. Austrian distribution grids are most vulnerable to grid congestion, followed by the Netherlands, while German grids are most robust seeing no overloads even with the highest modelled EV penetration.
- The grid performance impact factors including seasonal changes in load, PV and EV demand, weekday-weekend changes in EV demand, location of charging sessions (home, semi-public and public) as well as EV charger accessibility are investigated and discussed. All the above factors have not been dealt with together in previous works
- Grid performance is evaluated based on magnitude, duration and scale of the impact for node voltage drop, transformer and line loading as a function of increased EV penetration. The interrelation between the impact and the grid feature is also inspected.

The numerical results for these key observations are comparatively quantified using grid simulations and presented in the subsequent sections.

C. STRUCTURE OF THE PAPER

The simulation setup and the data-driven approach is in-detailed explained in Chapter II. The simulation results of three countries and three grid types are analysed in Chapter III. The study of grid performance impact factors including winter-summer, weekday-weekends, plus EV charger accessibility is also placed in Chapter III. The detailed interpretation over several grid performance key indicators is given in Chapter IV. Finally, Chapter V reports on the Study conclusions and recommendations for future work.

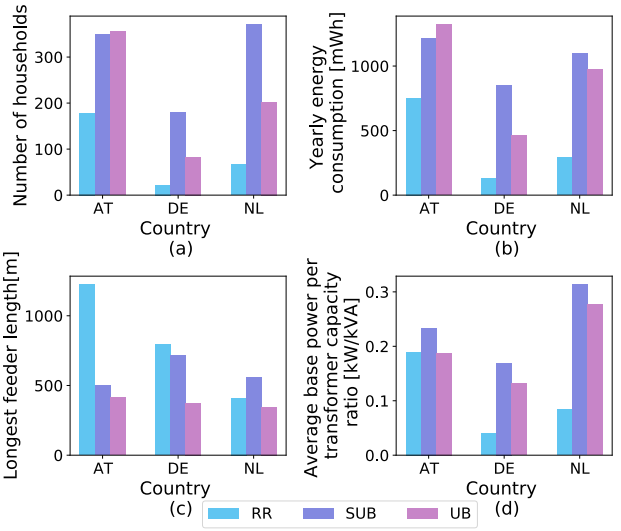

FIGURE 1. Comparison of basic grid features based on the 9 categories defined for the country and functional type (a) total number of households (b) yearly energy consumption (c) length of the longest feeder (d) the ratio of average baseload power with the total transformer capacity.

II. METHODOLOGY: DATA-DRIVEN APPROACH FOR REALISTIC GRID IMPACT EVALUATION

In this section, three layers of data-driven considerations of simulation input data are described, followed by the depiction of the simulation methodology as well as the output data.

1) Actual Grids segregated by (a) geography (b) function. (Section II-A)
2) Historical power profiles in the corresponding grid. (Section II-B)
3) EV charging data measured from chargers and survey-based car driving data pertaining to charging energy demand, arrival and departure time based on different charging session types. (Section II-C, II-D)

In each subsection, how the raw data was acquired and pre-processed are explained respectively.

A. GRID SPECIFIC DATA

Actual representative grids from three countries, namely, the Netherlands (NL), Germany (DE) and Austria (AT) are obtained from the Distribution System Operators (DSO). Further, three different functional grid types; rural (RR), suburban (SUB) and urban (UB); are considered. For each of these 9 categories, at least two test grid data per type per country is acquired, as summarized in Appendix A.

Fig. 1 compares the average values of the listed basic features based on 3 × 3 defined categories. The compared basic features are: total number of households (N_{hh}); yearly energy consumption (E_{yr}); length of the longest feeder, which is the length of the feeder from the transformer to the farthest end of the grid ($L_{\mathrm{f,max}}$), and the ratio ($\tau^{\mathrm{norm}}_{\mathrm{b,avg}} = P^{\mathrm{trafo}}_{\mathrm{avg}}/C^{\mathrm{trafo}}_{\mathrm{tot}}$) of average base load power ($P^{\mathrm{trafo}}_{\mathrm{avg}}$) with the total transformer capacity ($C^{\mathrm{trafo}}_{\mathrm{tot}}$). $\tau^{\mathrm{norm}}_{\mathrm{b,avg}}$ value is related to minimum reserve capacity and it can be used to identify which grids are relatively more vulnerable to overloading. In Fig. 2, all grids

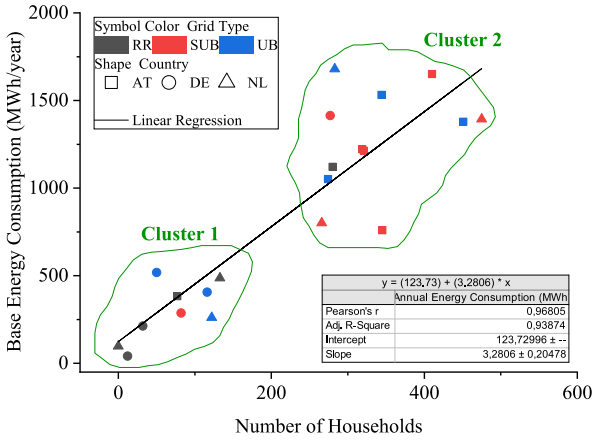

FIGURE 2. Clusters for base energy consumption as a function of the number of households for different category combinations of grid types and countries.

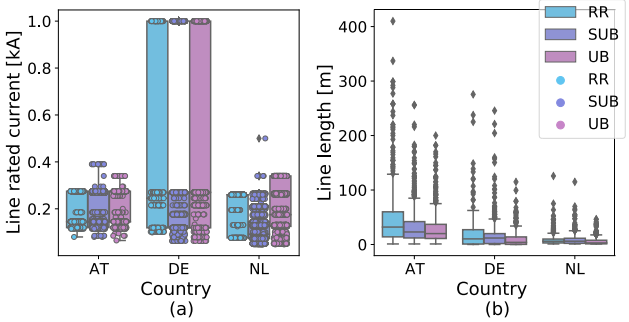

FIGURE 3. Grid line feature comparison between countries and grid types. (a) Line rated capacity in ampere (b) Line length in meter.

are clustered into two groups based on their number of households and yearly energy consumption. Cluster 2 grids have both high N_{hh} and E_{yr} values and Cluster 1 grids have relatively low N_{hh} and E_{yr} values. Most of the SUB grids and AT grids fall in Cluster 2 while the majority of RR grids, as well as DE grids, are in Cluster 1. The line features of each grid type in every country are also plotted and compared, which can be found in Fig. 3. Each dot in this box plot represents a line (cable) in the grids. Fig. 3 (a) shows the line rated current and it is clear that DE grids have a greater number of high-capacity lines compared to other countries. Similarly, the length of every line in each country is plotted in Fig. 3 (b). It can be observed that AT grids have relatively long lines and NL grids have shorter lines implemented.

Fig. 1-3 show that in general SUB grids have the highest N_{hh}, E_{yr} and $\tau^{\text{norm}}_{\text{b,avg}}$ relative to other functional categories for the given country. An out-liner to this trend are the N_{hh} and E_{yr} values of AT-UB grids, which are both slightly higher than the AT-SUB grids. Since EV penetration is assumed proportional to the N_{hh} in this paper, it can be inferred that an increase in serviced EVs for the given penetration level will be maximum for the SUB functional category. RR grids have the lowest N_{hh}, E_{yr} and $\tau^{\text{norm}}_{\text{b,avg}}$ across functional categories for any given country. Therefore, it is least prone to increase in EV penetration. However, RR grids have relatively high $L_{\text{f,max}}$ (NL grid is an out-liner). Therefore it is important to determine the minimum node voltage levels in these grids.

It can be inferred that for all functional category types, DE grids have maximum country-specific reserve capacity as indicated by lowest N_{hh}, E_{yr} and $\tau^{\text{norm}}_{\text{b,avg}}$. Furthermore, the number of serviced EVs per grid is lowest in DE for a given penetration level. In general, AT grids have the highest N_{hh}, E_{yr} and $\tau^{\text{norm}}_{\text{b,avg}}$ across functional categories, indicating lowest reserve capacity and a high number of serviced EVs for the given penetration. NL-SUB grids have the highest N_{hh} and therefore suggesting the highest increment in number of serviced EVs for the given penetration. At the same time, relatively high $\tau^{\text{norm}}_{\text{b,avg}}$ indicates a low reserve capacity in NL-SUB grids, making them vulnerable to transformer overloads. Furthermore, a significantly higher $L_{\text{f,max}}$ value for AT-RR grids suggests a wider spread of service area in these grids, thereby suggesting issues related to low node voltages are more likely in the former.

B. LOAD AND PHOTO-VOLTAIC (PV) PROFILES

In this study, the load and PV profiles were generated based on historical measurements or standardised profiles and the information of the unit, i.e. the load yearly energy consumption and the PV installation capacity.

The load energy consumption information of all three countries was provided together with the grid models by DSOs. The standardised load profile for Austria is available through AT Power Clearing & Settlement group [25], the standardised load profile for DE grids was obtained through the German Association of Energy and Water Industries, BDEW [26] and the standardised load profile for NL can be acquired from the Dutch Energy Data Exchange Association [27]. The standardised profiles are available for different load categories in each of the original data sources. For this study, three different categories are employed to model the baseload profiles. In Fig. 4, the load profiles of a load with 1000 kWh/year energy consumption are presented for all three countries. For AT and DE grids, the three used profile types are household, business and agriculture. The load categorisation is slightly different for NL grids in that they are distinguished by connection capacities, namely E1, E2 and E3 type groups. E1 types are small size connections that can be considered as households. E2 types are medium size connections with a different peak time compared to E1 types, and this type group is usually seen in small businesses like shops and companies. The E3 type group are other big capacity connections, for example, manufactures, farms. Fig. 4 not only compares the seasonal difference between different profiles but also shows the variations during weekdays and weekends. Almost all summer profiles are slightly smaller than the winter profiles except the business profile in AT. We can also see from this figure that business profiles in AT, DE and E2, E3 profiles in NL drop during the weekend. Therefore, the summer baseload is lower than the winter baseload for a certain grid. For a grid with more small business loads, a decreased weekend baseload could be expected.

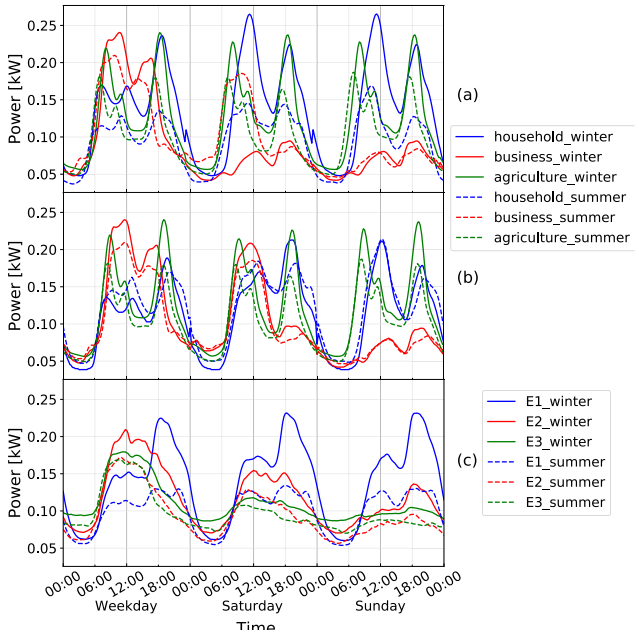

FIGURE 4. Standardised base load profiles with 1000 kWh yearly energy consumption of three countries, (a) AT, (b) DE, (c) NL.

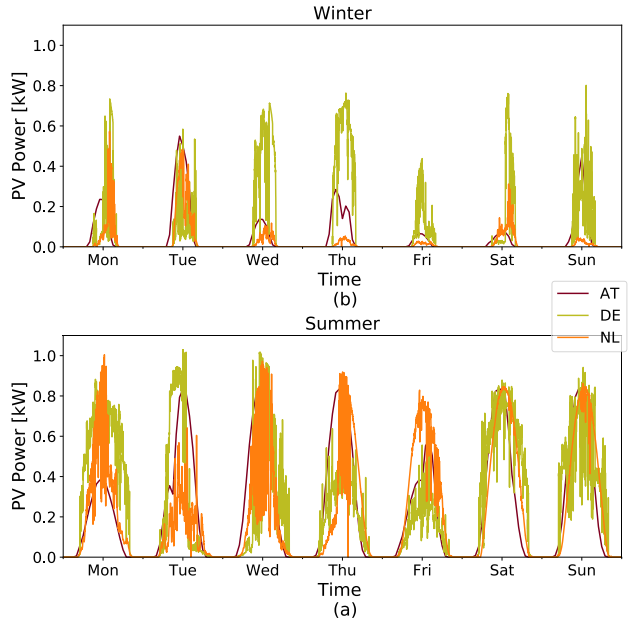

FIGURE 5. Standardised PV generation profiles with a 1kW peal rate of three countries (a) One sample winter week (b) One sample summer week.

For AT grids, the information of the installed PV is available in the grid models provided by Austrian DSO. The standardised PV profile was derived from weather data using the Python package PVwatts from NREL [28]. The raw standardised PV profile is in an hourly resolution, but an interpolation method was applied and the fluctuation of the per-minute PV power is introduced in the profile during the simulation. Similarly, the PV information including the location and capacity of installed PV systems is included in the DE grid models. The PV standard profile was generated by Meteonorm software, where ambient temperature and wind speed were considered and an optimal azimuth and tilt angle was assumed [29]. The PV installation information was not available via Dutch DSOs, thus an assumption was made based on the PV installation [30], [31] and the Dutch households [32] statistics. The PV installation assumption for NL grids is 25% PV penetration in RR grids, 15% PV penetration in SUB grid, and 5% PV penetration in UB grid where each installation has a 2.5 kW rated power. The PV penetration is calculated based on the number of loads in the grid. The standardised PV profile of NL is generated based on previous work [33]. The standard PV profile of all three countries with a 1 kW capacity installation in one summer week and one winter week is shown in Fig. 5.

TABLE 1. EV ownership distribution.

Car ownership distribution ($\alpha_{\text{car,hh}}$)		Grid type		
		RR	SUB	UB
Country	AT	1.5	1.35	0.75
	DE	1.6		
	NL	1.25	0.9	0.5

C. EV PENETRATION REPRESENTATION

In this study, the EV penetration levels 0%, 20%, 50% and 80% were simulated, where the EV penetration is defined as the percentage of total cars in a certain grid. The EV penetration level in simulations is handled in the form of the total number of charging sessions. The number of EVs in a certain grid is calculated as the product of the total number of households (N_{hh}), the car ownership distribution (car per household, $\alpha_{\text{car,hh}}$) and the EV penetration level (γ_{EV}), as shown in Eq. 1.

$$N_{\text{EV}} = N_{\text{hh}} \times \alpha_{\text{car,hh}} \times \gamma_{\text{EV}} \tag{1}$$

For all three countries, the number of households in the grid was provided by the DSOs. In AT models, car ownership is calculated based on the data of population, household size and the car per-capita registration data [34]. For NL, the car ownership data is assumed based on [35] and for DE the car ownership assumption data is provided by the German DSO. The summary of EV ownership distribution is shown in Table. 1

To simulate the impact of excessive charging demand caused by massive connected EVs, the total number of EVs in a certain grid needs to be converted to the corresponding EV charging sessions. The total EV charging sessions in a grid is calculated by its total number of EVs (N_{EV}) times the charging frequency ($\beta_{\text{sess,EV}}$), which is the average charging sessions per EV during a certain time period, as presented in Eq. 2.

$$N_{\text{sess}} = N_{\text{EV}} \times \beta_{\text{sess,EV}} \tag{2}$$

In addition, the charging sessions are categorised into three types namely home, semi-public and public, based on

TABLE 2. EV charging session distribution.

		Approach 1			Approach 2		
Raw data feature		Car mobility based			Charger measurement based		
Charge frequency ($\beta_{sess,EV}$)		0.9 per day			4 per week		
Grid type		RR	SUB	UB	RR	SUB	UB
Charging session distribution	Home	90%	98%	74%	70%	50%	25%
	Semi-public	5%	1%	15%	15%	25%	12.5%
	Public	5%	1%	11%	15%	25%	12.5%

their features like location of charging, time of arrival and duration of parking, as described in a previous study [36]. The charging sessions are then translated into different types of chargers to integrate into the grid simulation. Similar to local load and PV generation modelling, several data resources were used for EV charging demand modelling as well. Half of the EV demand data is based on the real measurement from EV chargers, so they are easy to be processed and ready to use. However, the other half of the raw EV demand data is based on real car driving statistics. This means extra steps are requested to convert these mobility data into EV charging demand. How these data were processed and implemented is explained in detail in the next section.

Due to the nature of the raw EV charging demand data, there were two approaches implemented to model the increasing EV penetrations in the grid. For car mobility based data, approach 1 is applied. In this approach, the chargers are placed at every household, workplace and shop node and the total number of chargers is fixed for all EV penetrations. The higher the EV penetration level is, the more charging sessions will occur, hence more chargers will be used. The average EV charging frequency of this approach is an outcome of the EV trip modelling, and the value is 0.9 times per day. With charger measurement based data, approach 2 is employed. Unlike approach 1, the number of chargers increases along with the EV penetrations in approach 2, but the location of the chargers in lower EV penetrations will not change for higher EV penetrations. This means the higher EV penetration scenarios are modelled by only adding new chargers on top of lower EV penetration scenarios. The average EV charging frequency of this approach is assumed to be 4 sessions per week per EV [37]. For both approaches, the charging sessions in lower EV penetration scenarios are preserved and the new charging sessions are added for higher EV penetration levels in a different format. This makes sure the only difference between different EV penetrations is the added new charging sessions for a certain grid. The summary of EV charging session distributions of both approaches is shown in Table. 2. How the charging profile of each charging session was modelled is introduced in the next section.

D. HISTORICAL MEASUREMENT-BASED EV FLEET AND DEMAND PROFILE GENERATION

The EV charging profile data consists of two parts, the EV fleet composition and the featured data of every charging session. Six to ten top-selling EVs in each country were

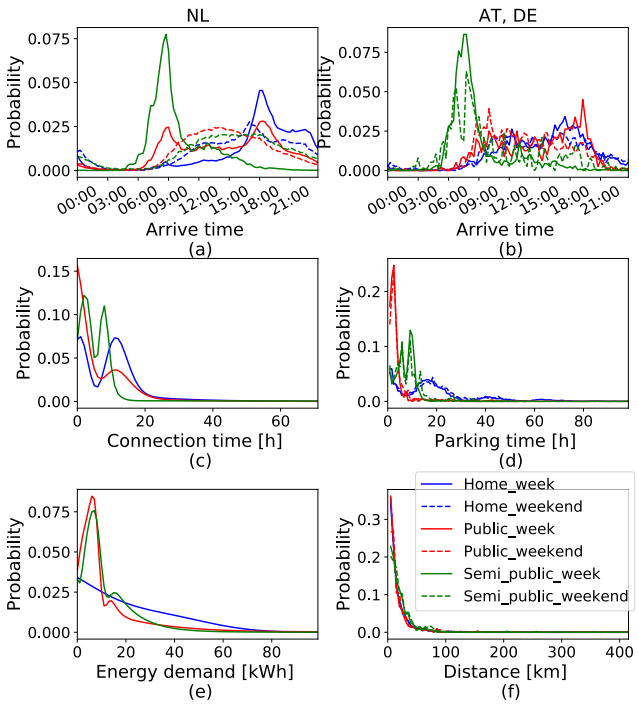

FIGURE 6. EV fleet demand probability distributions.

selected to compose the EV fleet based on their market data in 2018 separately [34], [38], [39]. As introduced in the previous section, the two raw EV data resources lead to two approaches of charging session modelling as well. Approach one needs extra steps to convert EV trip data into charging session data including EV arrival/departure time, EV arrival SOC and charging energy requests. While approach 2 models EV charging sessions directly from charger point of view based on the real charger measurements. Approach one was applied to all the AT grids and half of the DE grids while approach two was applied to the rest of the grids.

For approach 1, the mobility survey "Österreich Unterwegs 2013/2014" [40] conducted by the Austrian ministry of transportation serves as a good base for the probabilistic modelling of typical driving behaviour observed in rural, suburban and urban areas in Austria. This survey contains information on 196,604 trips which offers the time, frequency and distance distribution of the trips throughout the week. A Monte Carlo Approach as described in [41] was applied to generate specific trip data for each of the simulated electric vehicles by using the aforementioned EV fleet and trip data.

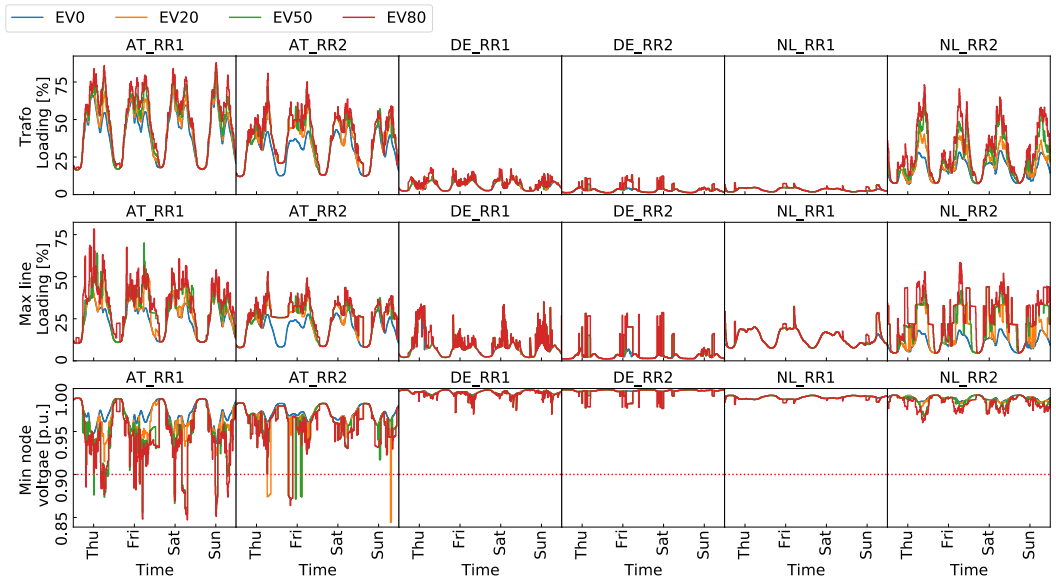

FIGURE 7. Loading of rural grids in winter.

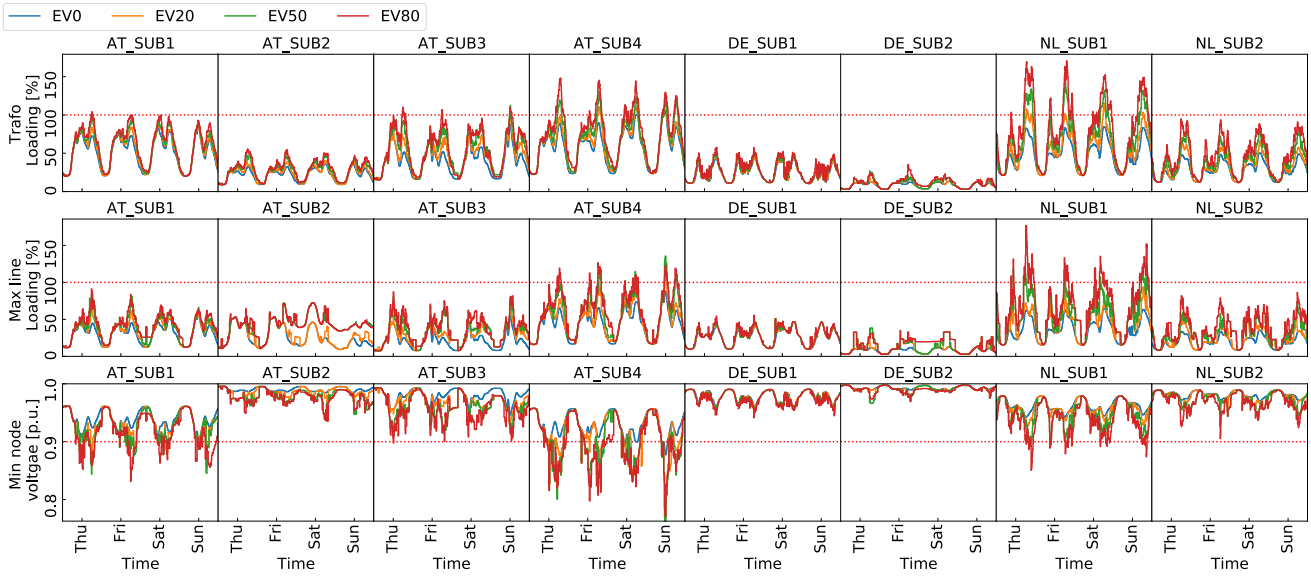

FIGURE 8. Loading of suburban grids in winter.

In the end, these trip data were translated into time, location, duration and charging energy information at the chargers.

Approach 2 simulates the charging sessions from the charger perspective and the employed data is based on a study conducted by ElaadNL [37], [42]. In this study, more than 1.5 million charging sessions were recorded and analysed, and the probability distribution of featured information of charging sessions including EV arrival time, parking duration and charged energy were provided. A Monte Carlo Approach was implemented to generate the charging session data based on the EV fleet as well as the charging session featured data. For both methods, several boundaries were set to ensure there are no anomalies in the generated data.

The probability distributions of EV charging session's arrival time, parking time and the energy demand/driven distance are presented in Fig. 6. All data is distinguished between weekdays and weekends except the EV parking and energy demand data in the Netherlands. The plot of NL EV arrival time distributions indicates that every type of charging session presents at least one of the morning/evening arrival peaks during the week, while the weekends' arrival times are mainly accumulated in the latter half of the day. Apart

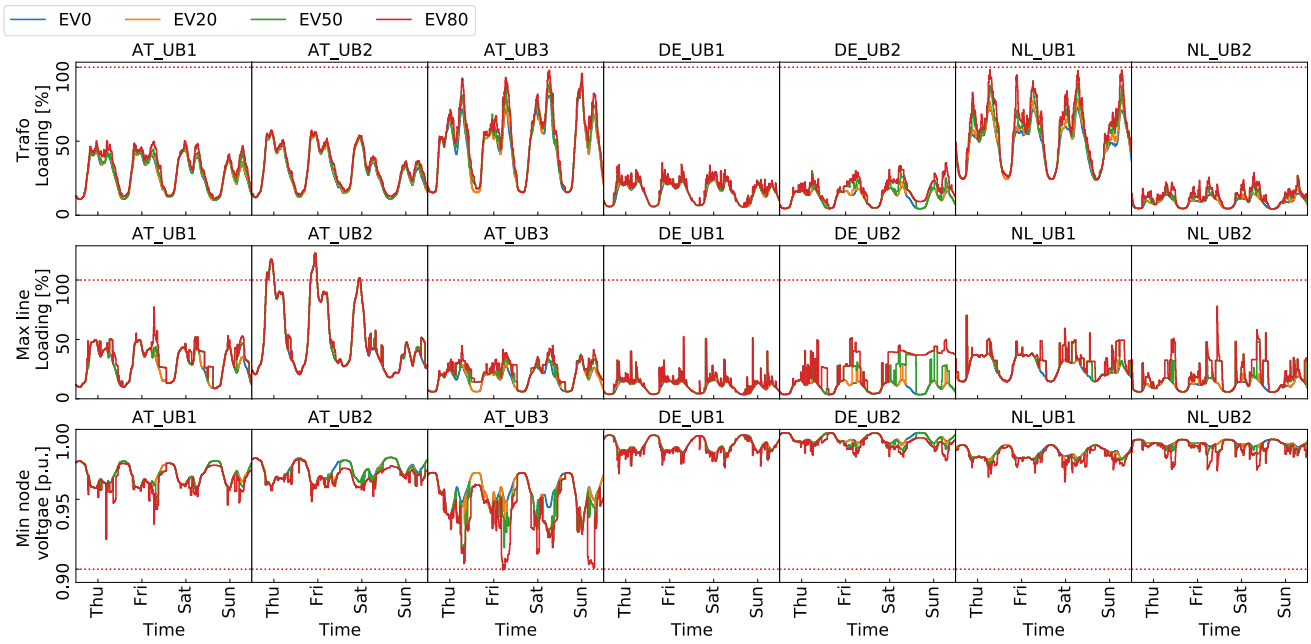

FIGURE 9. Loading of urban grids in winter.

from that, there is only minor weekday-weekends differences appeared in other distribution curves. Besides, the CC-CV charging stages of the battery were also considered in the charging profile modelling.

E. METHODOLOGY AND SIMULATION DATA

The simulations of this study were carried out with Python interfaced DIgSILENT-PowerFactory load flow simulations. A Python script was written to read input and modify the parameters in PowerFactory, then to initiate the load flow calculation at every time step. After every step of load flow analysis, the results were read and stored by this script as well. The input data for simulations are the aforementioned profiles. The raw output data of the load flow contains the loading/power/losses information of all the branches (including the transformer, the cables as well as the other link elements like fuses, impedance), and the voltage information of every node at every time step. All the EV chargers are modelled as constant power loads since it is our intention to see the consequence of all EVs being charged with their rated power without the influence of voltage drop at the end of the feeders. In this study, the overloading limit of transformer and lines are set to be 100% of their ratings and the under-voltage threshold is set as 0.9 p.u. [43]. The raw data was then processed and analysed referring to these limits.

It should be noted that even though the input information used for simulation is based on real data, it cannot cover all the possible situations in real life. The local load, PV generations and EV charging patterns are uncertain naturally. This study picked one possible combination and executed deterministic simulations to give an insight into the distribution grid performance under the influence of uncontrolled EV charging. Based on the there-layer data-driven considerations, the derived results of our paper are close to reality, and therefore the presented insight is useful.

III. SIMULATION RESULTS AND IMPACT FACTOR DISCUSSION

In this section, the simulation results are presented and compared. The possible impact factors of the results are analysed and discussed as well.

Fig. 7-9 show the results of transformer loading (top row), maximum line loading (middle row) and minimal node voltage (bottom row) versus time for three grid types in winter. The summer results can be found in Appx. V. The maximum line loading is the loading value of the most loaded line among the whole grid at each time step, and similarly, the minimal node voltage plot shows the voltage value of the lowest voltage node among the whole grid at every moment. For maximum line loading and minimal node voltage plots, the presented results are not from a specific line or node, but the worst recorded value among all the relevant elements of the grid as a whole.

From Fig. 7-9 we can see that transformer, line and node results show a similar trend in most cases. When the transformers experience high loading, the maximum line loading also has the tendency to increase while the minimal node voltage is more likely to have deep dips. These high loading moments usually occur on top of existing peaks that even without any charging EVs. This outcome is intuitive that the most uncontrolled charging moments occur during morning peaks when people charge their cars at work or

evening peaks when the users charge their cars once they are home. There are few occasions when the line loading or the node voltage do not share the same trend, for example, voltage drop in AT-RR grids, line loading in NL-RR2 and line loading in AT-UB2 grid. These phenomena were caused by local line overloading and regional voltage drop in remote areas of the grid.

A. RESULTS OF DIFFERENT GRID TYPES AND COUNTRIES

From Fig. 7 it can be noticed that none of the RR grids' transformers nor the lines are getting close to the overloading threshold. However, severe under-voltage problems already appear at some moment in both AT-RR1 and AT-RR2 grids with only 20% EV penetration. This under-voltage problem is purely caused by extremely long feeder length to the far-end of the grid, which is 1134 m and 1312 m separately. Besides, the EV charging adds a high level of extra loading to the RR grids that the transformer or line loading is doubled at some point even though the overall loading is within the limit.

The plots of SUB grids in Fig. 8 present dissimilar results in comparison to the RR grids. Half of the SUB grids bear different forms, magnitudes and duration of overloading. There are several reasons behind this effect. On average, the SUB grids especially AT and NL SUB grids, have high household numbers as well as a high baseload demand. On top of that, the car ownership per household is also considerable for SUB grids, which induces a high absolute number of EVs in SUB grids. In the end, the exorbitant overall load demand passes beyond the grid limits, which suggest that the potential of SUB grids for a high EV penetration is very restricted.

In Fig. 9, the simulation results of UB grids are displayed. The plots show that except for AT-UB2, all the other grids are within the congestion boundaries with very few moments being on the verge of the limit. The line congestion that occurs in the AT-UB2 grid is not because of EV charging, but due to the high grid baseload and the limit of the partial grid facility. A few cables in the grid are already overloaded with only baseload consumption, which strongly suggests an upgrade for these cables. It can be also seen from this plot that the EV charging does not add extensively extra loading to the grid. The near breach moments are largely due to the high baseload. There are two possible reasons for this outcome. In our simulation settings, urban grids do not have many households, thus the absolute number of EVs are not as high. Secondly, urban grids tend to have a compact layout where the line lengths are shorter in comparison to other grid types, as introduced in Fig. 3. With a compact layout, the node voltages are less likely to drop dramatically. Both factors lead to relatively less problematic results in urban grids. In all simulations, none of the DE grids had any congestion problem while a considerable ratio of AT grids experienced transformer, line overloading and under-voltage problems. For NL grids, the overloading and voltage drop issues only develop in SUB grids. The simulation results confirm with the inference in Section II-A.

One dominant reason of this outcome is the simulated DE grids have a relatively oversize-designed capacity compared to the other grids. This is signified by low N_{hh}, E_{yr} and $\tau_{\mathrm{b,avg}}^{\mathrm{norm}}$ values of DE grids, whilst more lines with higher capacity are possessed by DE grids as displayed in Fig. 1 to 3. The same mechanism falls on AT grids. Features of AT grids including high N_{hh}, E_{yr} values, long $L_{\mathrm{f,max}}$ and high ling length, suggesting they are more likely to encounter grid congestion issues in comparison with DE and NL grids. The simulation results show the corresponding tendency that a considerable ratio of AT grids experienced transformer (AT SUB1, SUB3, SUB4), line overloading (AT SUB4, UB2) and under-voltage problems (AT RR1, RR2, SUB1, SUB4, UB3).

B. IMPACT FACTOR DISCUSSION

To investigate factors that influence the EV integrated grid performance is also an objective of this paper. The impact of seasons, time of the week (weekday/weekends) as well as charger accessibility are discussed in this section.

1) SEASONAL AND TIME OF THE WEEK RESULTS VARIATIONS

The combination of PV generation, baseload and EV charging load affects the grid performance. Among these three inputs, baseload and EV charging load have weekday-weekend variations while PV generation and baseload deviate in different seasons.

The distribution analysis of all grid elements' loading values was performed and compared between the weekdays and the weekends. One analysis example is visualised in Fig. 10. The first two rows of this figure show the daily loading/voltage distribution of every element in this grid where the first row exhibits the weekday variations and the second row represents the weekend fluctuations. The weekday-weekends loading percentage difference distribution is illustrated in the last row of the figure. The colour of the curves in this figure depicts various quantile values of this distribution. For example, q1.5-q98.5 lines mean 1.5% and 98.5% quantile, and these two lines signify the 97% confidence interval. The min-max values are not plotted in this graph since they are already included in the previous results section.

For all three categories of AT and NL grids, the percentage difference between weekend-weekday loading shows a similar sinusoidal trend for all grid elements: the weekend loading is higher than the weekday loading in two time periods (during post-midnight hours before 6:00 and during the mid-day between 9:00 and 18:00), and the weekend loading is lower than the weekdays' during the rest of the day. The exact time windows as well as the magnitude of the weekend-weekday loading difference varies between countries and grid categories. The weekend-weekday percentage difference of DE grids deviates during the day but it still shares the same early morning trend where the weekend loading is lower.

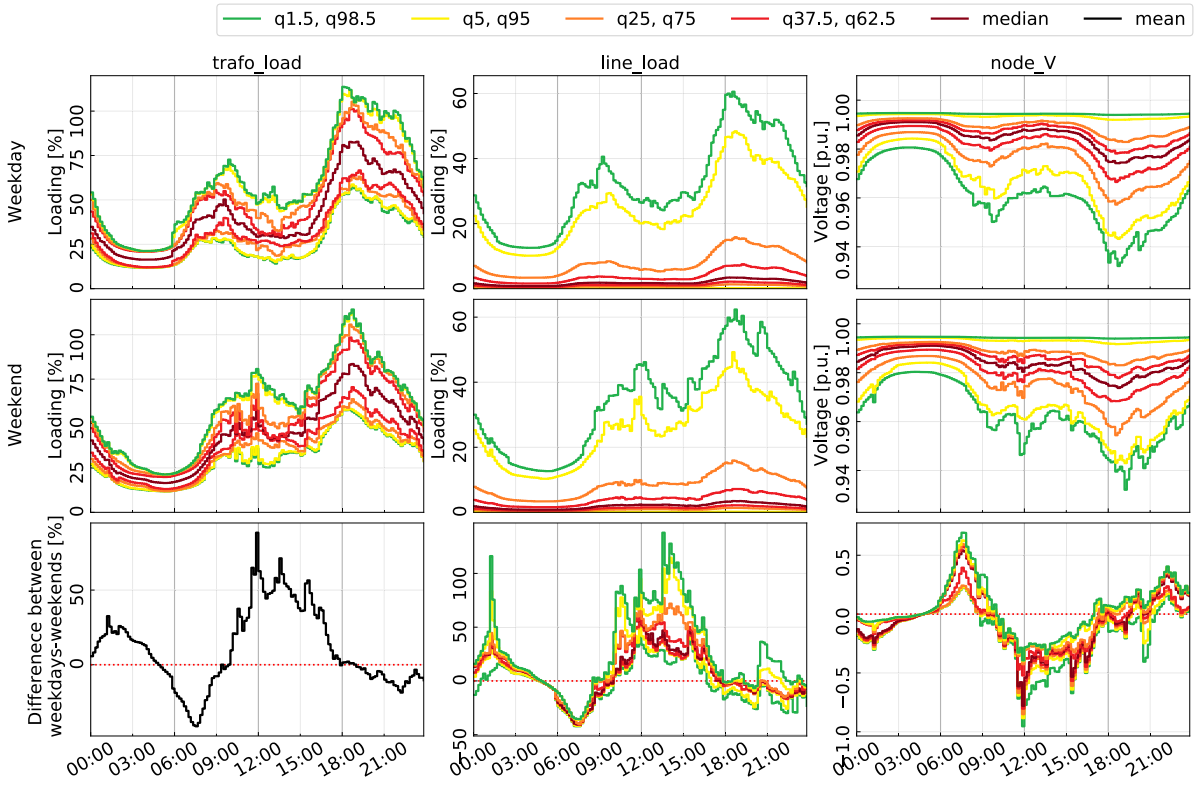

FIGURE 10. Loading distribution analysis between weekdays-weekends of AT SUB grids in winter.

This weekday-weekend loading difference is an outcome of a temporal and scale shifted demand in the weekend, especially for AT and NL grids. The daily morning demand starts to increase significantly from 6:00 during the weekdays, but this situation is alleviated during the weekends. The rising of morning demand is delayed to a later moment of the day and a higher morning peak is observed in the meantime. As a result, a higher loading during the day in comparison to the weekdays has developed. Concurrently, the evening demand peak of the weekend appears slightly earlier than on the weekdays, but the duration of the high evening load lasts longer than on the weekdays. This explains the shrink of the evening peak as well as the increment of the post-midnight loading. The loading shift shows a different pattern in DE grids that the weekend loading subsides around 9:00 - 18:00 in comparison to the weekday loading. Apart from that, there are no other conspicuous disparities between weekdays and weekends that can be summarised.

This shifted demand is contributed by the baseload oscillation and the diverted EV arrival time. From the baseload comparison graph Fig. 4 we can see that the household baseload (household profile for AT/DE grids and E1 profile for NL grids) has a delayed rising trend yet an elevated morning peak in the weekend. On the other hand, the business profiles (E2 profile for NL grids) encounter a considerable decline in weekends to different degrees during various time windows for all three countries. The EV arrival time probability distribution plots in Fig. 6 (a) & (b) clearly signify the EV start charging time discrepancy between the weekdays and weekends. Since this study investigates an uncontrolled EV charging scheme, the EV arrival time equals the EV charging start time. The weekend EV arrival time in NL congregates with a mild ramp between 9:00 and 23:00 instead of clustering around morning and evening peaks at 9:00 and 18:00 respectively. Similarly, the weekend charging start time of AT and DE EVs happen less in both morning and evening peaks but more during the day between 9:00 and 18:00.

As introduced in Section II-B, grids with more business/factory/agriculture types of loads have the tendency of experiencing less loading during the weekend. It is also suggested in Section II-D that there are lower EV charging peaks at weekends thanks to the spread-out arrival time distributions with a smoother ramp during the weekend. Even though some grids for instance AT-RR2, NL-SUB1, AT-SUB1 and DE-UB1 indeed have less severe loading during the weekend, the congestion level difference between weekdays and weekends is inconsequential.

In this study, only a one-week length of simulation was conducted thus the observed weekday-weekends differences have their limitations. It is encouraged to explore more weeks throughout the whole year in future research.

For the difference between seasons, it is not surprising to see that all grids bear notably fewer congestion issues in Summer than in Winter. This change is caused by a lower load demand and a higher PV generation in summer along with a nonseasonal distinguished EV demand, which is indicated in Fig. 4-6. The employed EV input data in this paper does not characterise seasonal deviations, but it is interesting to consider in future studies.

2) IMPACT OF CHARGER ACCESSIBILITY

There is one interesting effect that can be noticed in the simulation results, which is the branch loading and the voltage drop for 20% and 50% EV penetrations are worse than the 80% penetration case of some grids. For example, the last day of transformer loading in AT-SUB3, the second day of node voltage and line loading in DE-SUB2 and the node voltage of AT-RR2.

This phenomenon is specific to the way the simulation was set up and how the EV charging demand was modelled. EV charging demand modelling Approach 1 fixes the number of chargers in the grids and models the EVs charging sessions proportional to the EV penetration as explained in Section II-C and II-D. This EV penetration increment modelling method introduces a situation when a new earlier charging session in a higher EV penetration scenario is added on top of an existing later charging session in the lower EV penetration scenario. If these two charging sessions happen to occur at the same location and within the same time window, a charging request overlap situation happens. Under this circumstance, the later session from the lower EV penetration scenario can no longer take place as planned when the earlier session from the higher EV penetration scenario occupies the charging slot. This leads to two outcomes, one is the later arrived EV waits in the queue for the already connected EV to finish. Alternatively, if there is a nearby available charging slot, the later arrived EV should move to a different slot. Hence, if the later charging session causes the overloading in lower penetration scenario could not happen due to an earlier session in higher EV penetration scenario, the worse overloading in lower EV penetration phenomenon occurs. This overlapping situation appeared several times in the simulation and it led to a slightly different EV charging profile even for the exact same charging session and eventually reflected in the grid loading results.

This queue mechanism induced by charging session overlap has a two-edged effect. It can passively reduce the potential congestion that new peaks will not be added infinitely to the existing peaks thanks to the physical limitation of available charging points. On the other hand, the queue effect can also increase the peak loading, if the delayed EV charging moves into another peak period or is connected to another slot located at the overloaded region. EV charging demand modelling Approach 1 mimics a situation where there is limited charger accessibility to the number of EVs. Differently, the EV demand modelling Approach 2 imitates another situation where there are enough charge points and they are always available for any EV to be charged whenever and wherever there is a request. This situation can lead to a circumstance where the charging demand happens during the peak time stack on each other without any limitation, resulting in an extremely high grid loading peak. One typical example is the transformer loading of day one in NL-SUB1 (Fig. 8).

This difference in the loading peaks is an outcome of how the EV demand is modelled, showing that whether there are enough chargers to the corresponding number of EVs can affect problems occurring at the node level for a very realistic setup.

IV. COMPARISON OF DIFFERENT GRID BEHAVIOUR WITH KEY INDICATORS

To better understand to what degree the grid congestion problems occur and what the influential factors are, several evaluation indexes are used to analyse the results.

A. THE MAGNITUDE OF GRID CONGESTION

Fig. 11 and Fig. 12 show the amplitude of grid congestion with maximum loading values in descending order and minimum voltage values in an ascending order together with relevant grid features. The values in both figures are sorted based on the 80% EV penetration winter results, which are indicated by the black dash boxes. The common grid features for both plots are total yearly energy consumption (E_{yr}) and number of households (N_{hh}). Larger or higher density grids (higher E_{yr} and N_{hh}) have a tendency to experience more grid congestion issues. Apart from grid dimension, the ratio of average baseload power and the total transformer capacity ($\tau^{\mathrm{norm}}_{\mathrm{b,avg}}$) also relate to higher transformer and line loading. The average line ratings ($r_{\mathrm{l,avg}}$) instead do not show a strong connection with the line loading trend. However, for minimal node voltage, a clear association appears between the decreased minimal node voltage and the combination of average line length ($L_{\mathrm{l.avg}}$) and the longest feeder length ($L_{\mathrm{f,max}}$). The winter and summer results comparison has an expected effect that the grid congestion problem is milder in summer.

NL-SUB1 grid has the highest transformer and line peak loading and the highest loading growth caused by EV charging for two possible reasons. One is the grid feature, that NL-SUB1 has the highest N_{hh}, the lowest $L_{\mathrm{l.avg}}$ and the second highest $\tau^{\mathrm{norm}}_{\mathrm{b,avg}}$ values among all the grids. Another reason is related to how the EV charging profile is modelled, as previously mentioned in Section III-B2. The EV charging demand in NL grids was modelled with Approach 2 (charger approach), and the increased EV penetration is reflected as the increasing number of chargers. Any newly added EV in the grids has a guaranteed charging spot without having to wait in the queue during the busy time, unlike in the AT grids. This induces that all the EV charging requests will take place without delaying and leading to an extremely high loading peak.

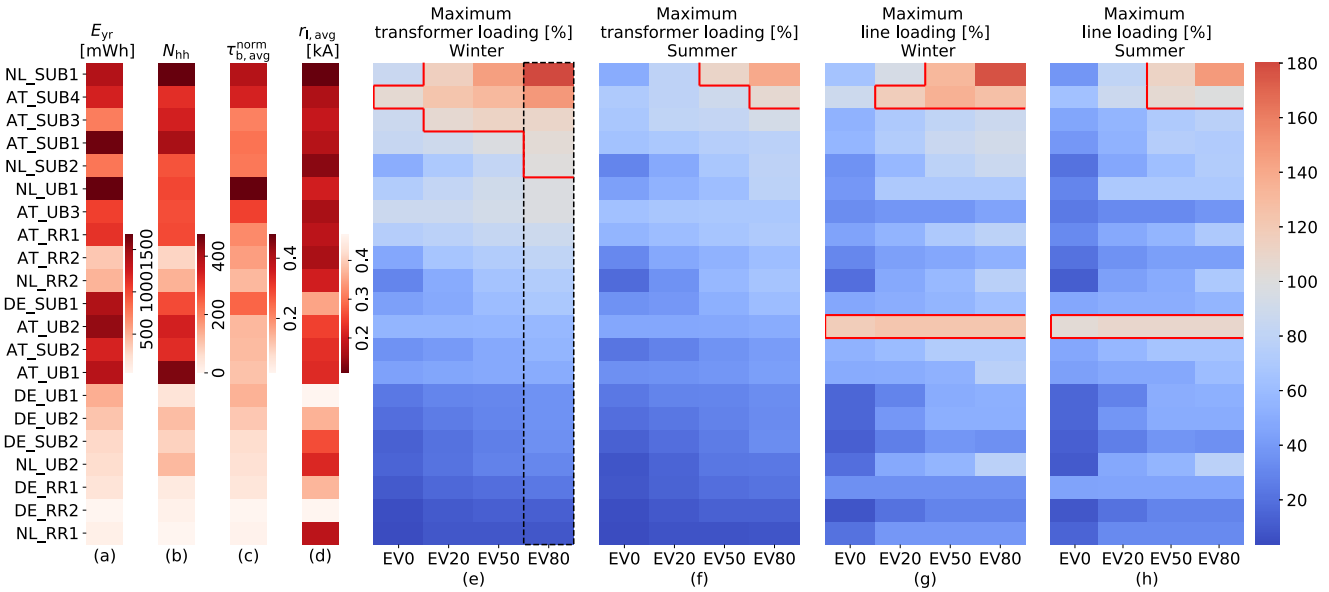

FIGURE 11. Heat map of maximum transformer and line loading in both seasons.

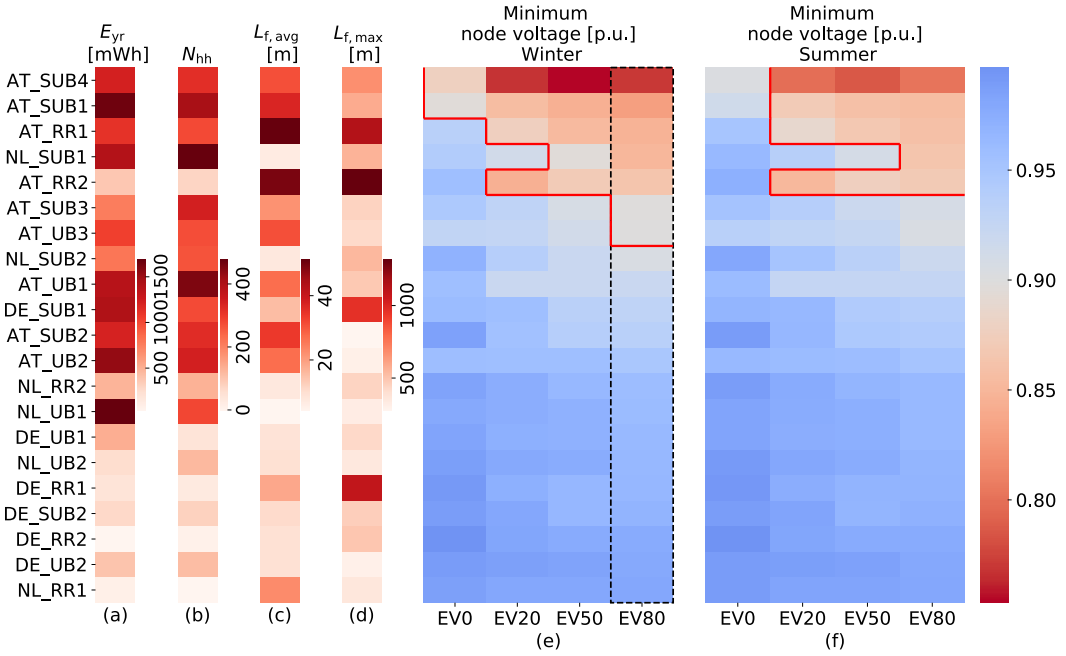

FIGURE 12. Heat map of minimal node voltage in both seasons.

The results where congestion problems present are circulated with red lines and it shows the ratio of problematic grids caused by EV uncontrolled charging is moderate, but the magnitude of overloading is significant for two SUB grids. Besides, there are more grids that have under-voltage problems than the number of grids with transformer and line overloading issues. Moreover, two out of seven under-voltage risk grids already suffer from under-voltage problems in winter even without EV charging and clearly, excessive EV demand does not help with the situation.

B. DURATION AND SCALE OF THE GRID CONGESTION

To study the duration and scale of the congestion issues, Fig. 13ii and 14 are displayed. In Fig. 13ii, the ratio of overloaded energy ($E_{\text{ol,xmer}}$) and overloaded time ($t_{\text{ol,xmer}}$) are presented and how they are calculated is explained in Fig. 13i. Two SUB grids experience up to 30% of transformer overloading duration as well as overloaded energy, which indicates these two grids request immediate attention, for example, charging scheduling or grid facility upgrades with even low EV penetration levels. Similarly, the scale of

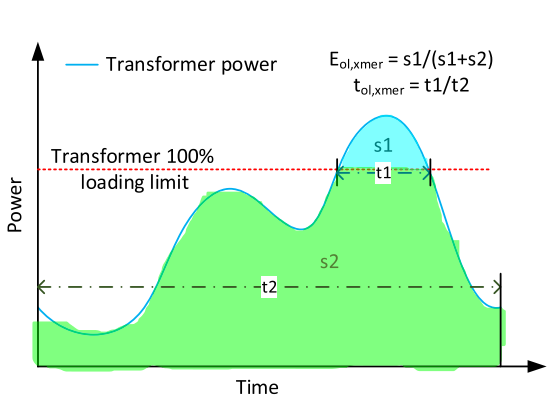

(i) Calculation explanation of overloaded energy and time ratio

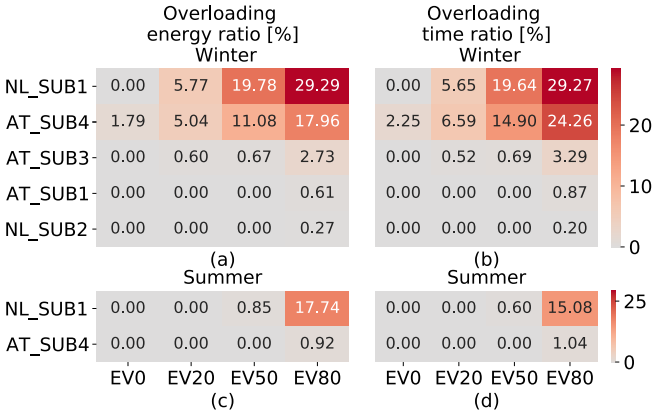

(ii) Heat map of grid congestion duration index: overloaded energy and time ratio

FIGURE 13. **Duration and quantity of transformer overloading visualisation.**

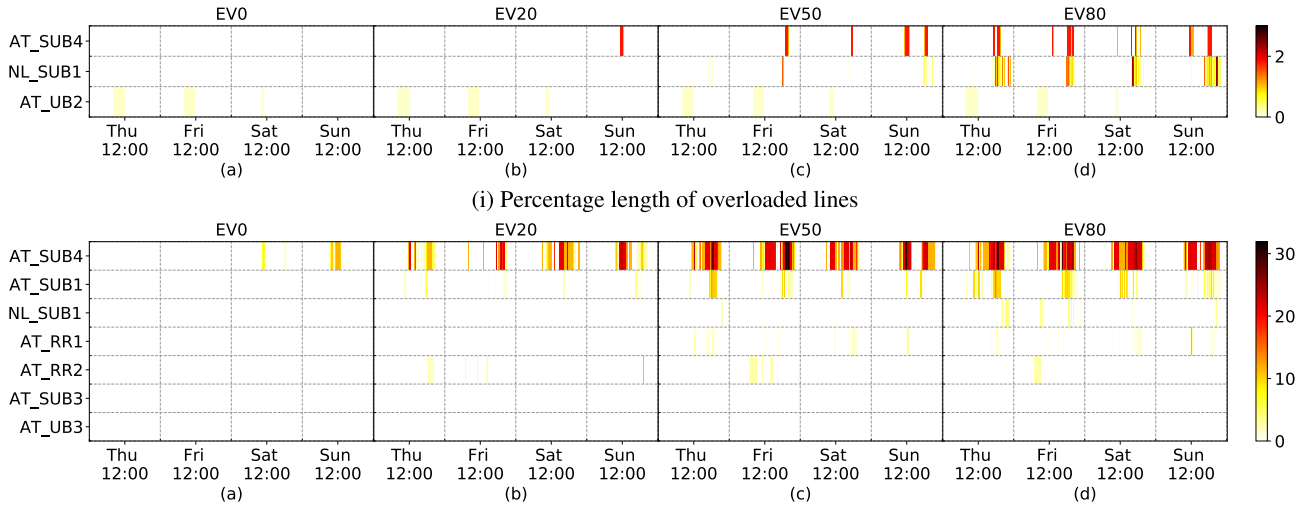

(i) Percentage length of overloaded lines

(ii) Percentage number of under-voltage nodes

FIGURE 14. **Heat map of grid congestion scale in Winter. For both figures: (a) 0% EV (b) 20% EV (c) 50% EV (d) 80% EV.**

line congestion and node under voltage is presented in the format of percentage length of overloaded lines ($L_{\text{ol,line}}$) and percentage number of under-voltage nodes ($N_{\text{uv,node}}$) respectively.

$$L_{\text{ol,line}} = \frac{\sum_{i=1}^{M_{\text{tot,l}}} l_{i,ol}}{\sum_{i=1}^{M_{\text{tot,l}}} l_i}, \quad l_{i,ol} = \begin{cases} l_i & \text{if line i} \\ & \text{is overloaded} \\ 0 & \text{otherwise} \end{cases} \tag{3}$$

$$N_{uv,node} = \frac{\sum_{i=1}^{N_{\text{tot,n}}} n_{i,uv}}{N_{\text{tot,n}}}, \quad n_{i,uv} = \begin{cases} 1 & \text{if node i} \\ & \text{under-voltage} \\ 0 & \text{otherwise} \end{cases} \tag{4}$$

How $L_{\text{ol,line}}$ and $N_{\text{uv,node}}$ are calculated are described by Eq. 3 and Eq. 4 respectively, where $M_{\text{tot,l}}$ is the total number of lines, $N_{\text{tot,n}}$ is the total number of nodes and l_i is the length of line i. The variation of $L_{\text{ol,line}}$ and $N_{\text{uv,node}}$ versus time is shown in Fig. 14 with an ascending order in y axis.

A maximum less than 3% $L_{\text{ol,line}}$ value reveals the scale of line overloading is rather small that it only occurs at several featured lines. These lines are either central lines connected close to the transformer or local lines connected to high consumption loads. On the contrary, AT-SUB1 and AT-SUB4 have significantly high $N_{\text{uv,node}}$ values. Especially for AT-SUB4, at least one-fifth of the grid is having under-voltage problems during almost half of the simulation time in 80% EV penetration scenario. This outcome pinpoints again that voltage drop is a fierce issue that needs to be solved in distribution grids. A small improvement on the facility, for example, a reconfiguration of the tap positions of the transformer, might already help with the situation.

TABLE 3. Summary of grid performance.

	Transformer loading		Line loading			Node voltage		
	Magnitude	Duration	Magnitude	Duration	Scale	Magnitude	Duration	Scale
AT-RR					***	**	**	
AT-SUB	**	***	***	**	*	***	***	***
AT-UB			**	*	*	*	*	*
DE-RR								
DE-SUB								
DE-UB								
NL-RR								
NL-SUB	***	***	***	***	*	**	**	*
NL-UB								

More number of "*" means the problem is more severe

TABLE 4. Summary of all grids' characteristics.

Grid	No. households	Yearly energy consumption[Mwh]	Avg. line length [m]	Longest feeder length [m]	No. transformer & capacity [kVA]
AT-RR1	280	1121.0	51.0	1134.0	1×630 kVA
AT-RR2	77	384.0	49.0	1312.0	1×250 kVA
AT-SUB1	410	1651.0	37.0	590.0	2×400 kVA
AT-SUB2	321	1213.0	34.0	280.0	1×400+1×630 kVA
AT-SUB3	345	760.0	22.0	457.0	1×400 kVA
AT-SUB4	319	1222.0	31.0	678.0	1×400 kVA
AT-UB1	451	1379.0	27.0	491.0	2×630 kVA
AT-UB2	344	1532.0	27.0	314.0	2×630 kVA
AT-UB3	274	1052.0	31.0	431.0	1×400 kVA
DE-RR1	32	213.5	18.9	1087.0	1×400 kVA
DE-RR2	12	42.0	10.0	499.987	1×250 kVA
DE-SUB1	277	1414.0	15.8	962.4	1×630 kVA
DE-SUB2	82	287.0	11.0	471.545	1×400 kVA
DE-UB1	50	518.0	9.5	436.672	1×400 kVA
DE-UB2	116	406	10	312.2	1×400 kVA
NL-RR1	3	98.0	22.8	367.8	1×400 kVA
NL-RR2	133	486.8	7.9	452.2	1×400 kVA
NL-SUB1	475	1394.1	7.3	566.0	1×400 kVA
NL-SUB2	266	800.8	8.1	546.6	1×400 kVA
NL-UB1	283	1680.2	4.4	332.5	1×400 kVA
NL-UB2	122	261.0	10.3	360.4	1×400 kVA

C. KEY TAKEAWAY

With the in-depth index comparison and analysis, it can be concluded that the majority of the grids do not face major congestion when penetrated with 50% EVs. Most of the problematic grids have a small scale and short duration of grid limit breaching. However, under-voltage is a problem worthy of attention, not only because more grids have higher magnitude, longer duration and bigger scale of voltage drop, but also because the voltage drop has a high vacillation rate on many occasions. Besides, a study [44] found that upgrade grid facilities, for example, the transformer capacity has very limited improvement on the voltage drop caused by a large amount of EV charging. That leaves less option for accommodating massive EV charging in LV grids, but on the other hand, it opens the opportunity to look into alternative methods, for example, smart charging scheduling, apart from the grid facility upgrades. It is an interesting aspect to research in future work.

V. CONCLUSION AND RECOMMENDATION

In this research work, the performance of 21 grids from three countries (Austria, Germany, Netherlands) with four EV penetration levels (0, 20, 50, 80%) in two seasons (Winter, Summer) are analysed and several interesting points are discussed. This paper focuses on the grid performance comparison along with EV penetration levels, between countries, and of different grid types. The other impact factors including seasons, time of the week (weekdays or weekends) and charger accessibility are also studied. Several key indicators of the magnitude, duration and scale of the grid congestion aree examined. The overall performance of all grids is summarised in Table. 3.

The grids from all three countries share a few similarities. First, the loading of transformer and lines, as well as minimal node voltage, share similar trends and the extra loading contributed by EV uncontrolled charging are predominantly added on top of the existing peaks. This phenomenon is rather apparent as most of charging events occur when the users come to work (morning peak) or get back home (evening peak). Secondly, the SUB grids in all three countries tend to endure more congestion issues in comparison to other grid types. This is because all SUB grids in the simulation have the highest household numbers as well as a relatively high car ownership ratio. This leads to a higher baseload

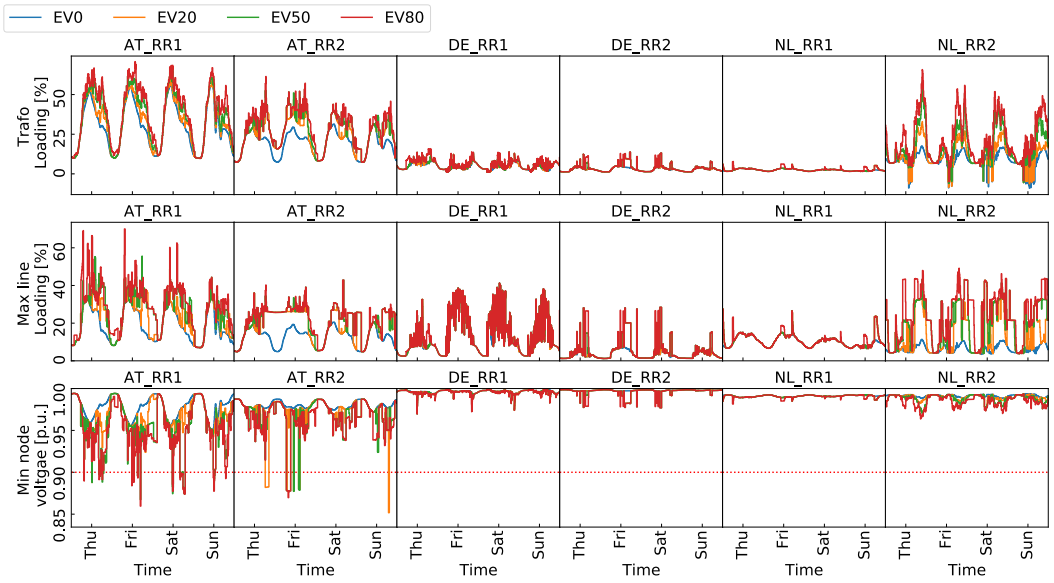

FIGURE 15. Loading of rural grids in summer.

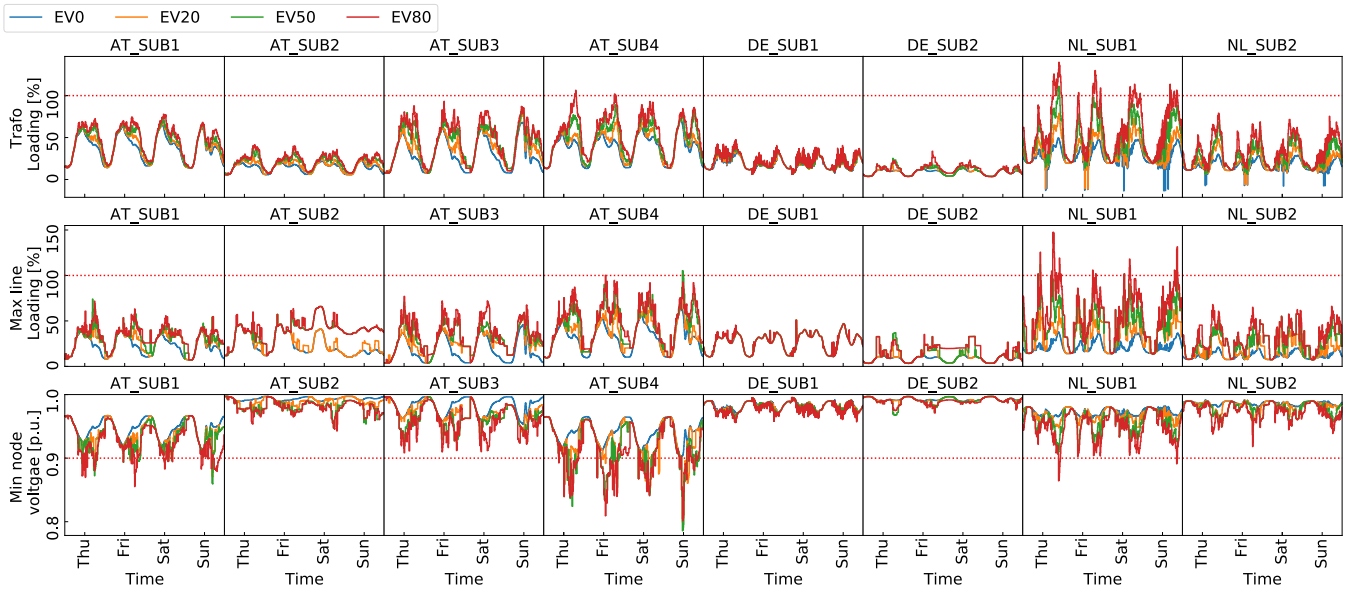

FIGURE 16. Loading of suburban grids in summer.

consumption as well as an increased number of EVs which causes a higher total demand in comparison to RR and UB grids. Thirdly, partial loading of the grid shifts from early morning and evening towards the middle of the day on weekends. Even though some grids like AT-RR2 do encounter a slightly reduced loading during the weekends, the disparity of congestion level between weekdays and weekends is insignificant. Finally, all grids have fewer overloading issues in the summer compared to the winter because of a lower baseload consumption while receiving a higher PV generation.

The grid performance in each country also has its own characteristics. All simulated DE grids are designed with higher redundant capacities, therefore none of them had any issue in all the simulations. AT grids have the highest incidence of congestion problems. Apart from SUB grids, AT-RR grids which have both transformer and lines operating well within the safe range still confront the risk of voltage drop below 0.9 p.u., with even 20% EV penetration, due to their excessively long longest feeder's length. NL-SUB1 grid has the highest transformer and line peak loading problem not only because of the grid features and the EV penetration

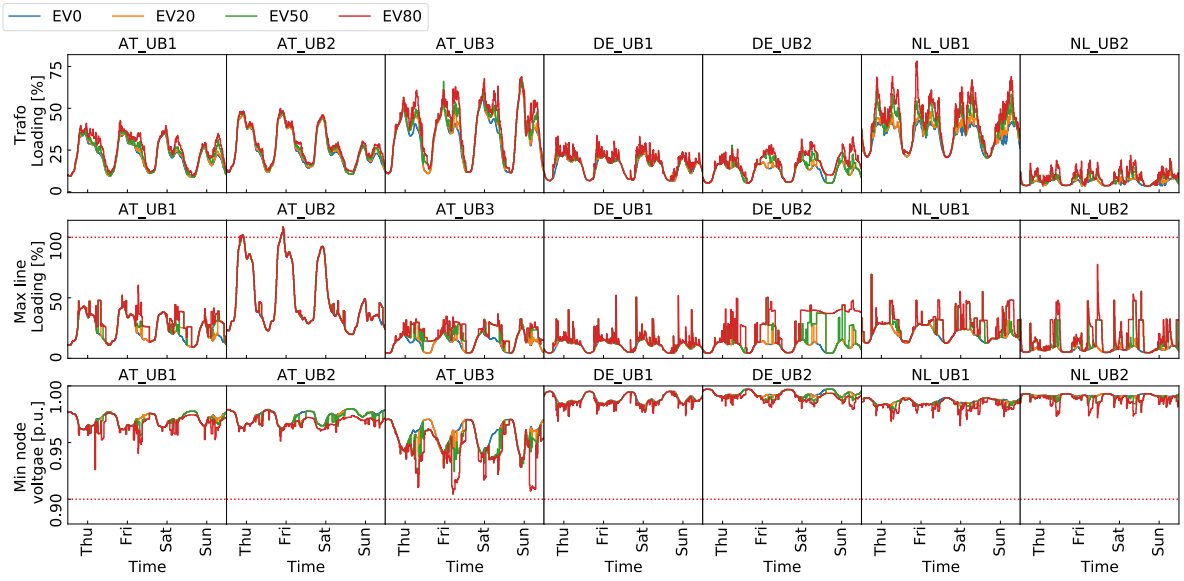

FIGURE 17. Loading of urban grids in summer.

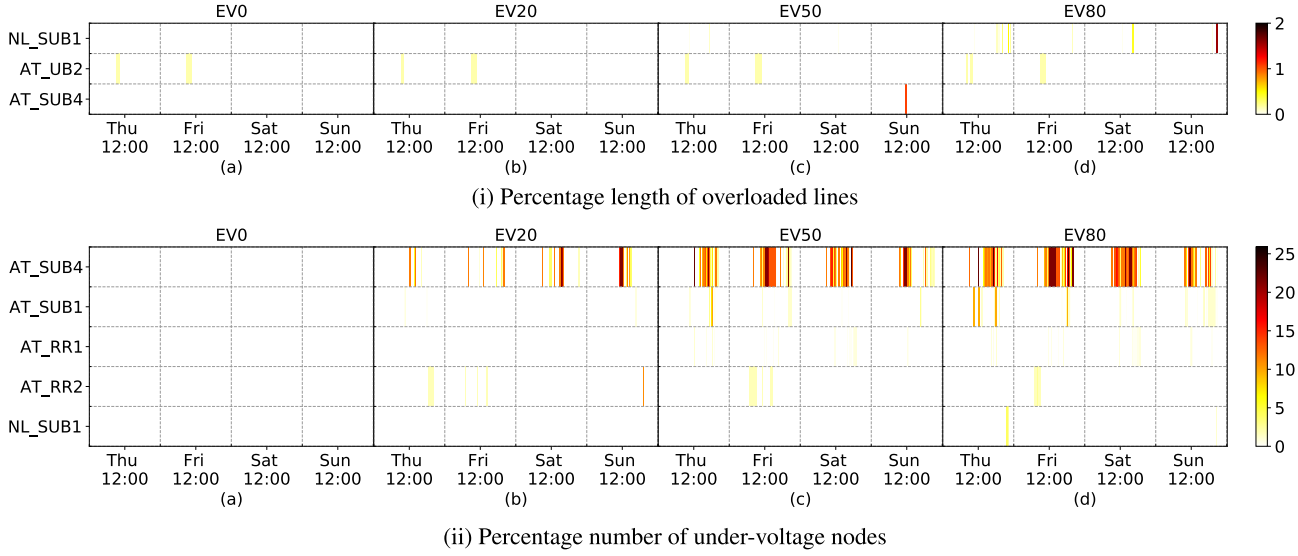

(i) Percentage length of overloaded lines

(ii) Percentage number of under-voltage nodes

FIGURE 18. Heat map of grid congestion scale in summer. For both figures: (a) 0% EV (b) 20% EV (c) 50% EV (d) 80% EV.

level but also related to how the EV charging demand were modelled. The difference in simulation results due to two EV charging session modelling approaches regarding "EV penetration versus the available number of charging points in the grid" inspires future research ideas. Whether charging points should be installed or not and how many are in view of increasing EV penetrations is critical to investigate further.

Thirteen out of twenty-one simulated grids encounter no congestion in any form even with an 80% EV penetration level. Most of the congestion has a relatively short duration on a small scale, where smart charging scheduling is needed, and a good result can be expected. However, one NL-SUB grid and two AT-SUB grids showed massive transformer loading and voltage drop problems in both amplitude and scale manner, indicating a possible hard violation on the grid facility upper limit. Regarding the severe problematic grids, two possible solutions are desirable to investigate in future work. One is to develop a smart charging method to reschedule the crowded charging process and optimise the grid capacity usage. Another one is to identify the most susceptible point in the grid and upgrade the related facility.

Even though this uncontrolled EV charging impact study advocate a rather optimistic outcome regarding distribution grids integrated with high EV penetration levels, there are a few things shall be noted. All the baseloads implemented in the study are standardised load profiles, which are averaged

and smoothed from real measurements. These standardised load profiles do not contain high-frequency power spikes and therefore do not accurately reflect the real baseload fluctuations. Because of this, grids might face the risk of higher congestion in situ, especially since short moments of grid limits breach might occur more readily when the same level of EV penetration as in the simulations is accommodated. Besides, all the EV penetration calculations were based on the car ownership registration but not the actual car parking information. In reality, the location of car registration might be far removed from regular charging spots. Therefore, the EV commute and how the commute alters the EV distribution between different LV grids are worth investigating in the future.

Despite the simplification during the modelling and the data pre-processing, this paper provides an insight into the uncontrolled EV influenced grid performance from different angles. The results of this study reflect what degree the EV uncontrolled charging overburdened the grids and what are the relevant impact factors, thus offering a valuable reference concerning future planning for DSOs.

APPENDIX A
GRID CHARACTERISTICS

See Table 4.

APPENDIX B
SUMMER RESULTS

See Figures 15–18.

ACKNOWLEDGMENT

The authors would like to thank three DSOs for providing the grid data: Vorarlberger Netz (AT), EWE NETZ (DE), Enexis (NL). The authors would also like to thank the project partner ElaadNL for their support in EV charging data.

REFERENCES

[1] K. J. Dyke, N. Schofield, and M. Barnes, "The impact of transport electrification on electrical networks," *IEEE Trans. Ind. Electron.*, vol. 57, no. 12, pp. 3917–3926, Dec. 2010.

[2] K. Clement-Nyns, E. Haesen, and J. Driesen, "The impact of charging plug-in hybrid electric vehicles on a residential distribution grid," *IEEE Trans. Power Syst.*, vol. 25, no. 1, pp. 371–380, Feb. 2010.

[3] S. Shafiee, M. Fotuhi-Firuzabad, and M. Rastegar, "Investigating the impacts of plug-in hybrid electric vehicles on power distribution systems," *IEEE Trans. Smart Grid*, vol. 4, no. 3, pp. 1351–1360, Sep. 2013.

[4] S. M. Elnozahy and M. A. M. Salama, "A comprehensive study of the impacts of PHEVs on residential distribution networks," *IEEE Trans. Sustain. Energy*, vol. 5, no. 1, pp. 332–342, Jan. 2014.

[5] J. Xiong, K. Zhang, Y. Guo, and W. Su, "Investigate the impacts of PEV charging facilities on integrated electric distribution system and electrified transportation system," *IEEE Trans. Transport. Electrific.*, vol. 1, no. 2, pp. 178–187, Aug. 2015.

[6] M. A. Awadallah, B. N. Singh, and B. Venkatesh, "Impact of EV charger load on distribution network capacity: A case study in Toronto," *Can. JElect. Comput. Eng.*, vol. 39, no. 4, pp. 268–273, Fall 2016.

[7] *Electric vehicle conductive charging system—Part 1: General requirements*, Standard IEC 61851-1, 2010.

[8] H. Turker, S. Bacha, and A. Hably, "Rule-based charging of plug-in electric vehicles (PEVs): Impacts on the aging rate of low-voltage transformers," *IEEE Trans. Power Del.*, vol. 29, no. 3, pp. 1012–1019, Jun. 2014.

[9] M. K. Gray and W. G. Morsi, "Power quality assessment in distribution systems embedded with plug-in hybrid and battery electric vehicles," *IEEE Trans. Power Syst.*, vol. 30, no. 2, pp. 663–671, Mar. 2015.

[10] M. F. Shaaban, Y. M. Atwa, and E. F. El-Saadany, "PEVs modeling and impacts mitigation in distribution networks," *IEEE Trans. Power Syst.*, vol. 28, no. 2, pp. 1122–1131, May 2013.

[11] C. Jiang, R. Torquato, D. Salles, and W. Xu, "Method to assess the power-quality impact of plug-in electric vehicles," *IEEE Trans. Power Del.*, vol. 29, no. 2, pp. 958–965, Apr. 2014.

[12] A. S. B. Humayd and K. Bhattacharya, "A novel framework for evaluating maximum PEV penetration into distribution systems," *IEEE Trans. Smart Grid*, vol. 9, no. 4, pp. 2741–2751, Jul. 2018.

[13] K. Qian, C. Zhou, M. Allan, and Y. Yuan, "Modeling of load demand due to EV battery charging in distribution systems," *IEEE Trans. Power Syst.*, vol. 26, no. 2, pp. 802–810, Mar. 2010.

[14] R.-C. Leou, C.-L. Su, and C.-N. Lu, "Stochastic analyses of electric vehicle charging impacts on distribution network," *IEEE Trans. Power Syst.*, vol. 29, no. 3, pp. 1055–1063, May 2014.

[15] L. Pieltain Fernández, T. Gómez San Román, R. Cossent, C. M. Domingo, and P. Frías, "Assessment of the impact of plug-in electric vehicles on distribution networks," *IEEE Trans. Power Syst.*, vol. 26, no. 1, pp. 206–213, Feb. 2011.

[16] E. Mancini, M. Longo, W. Yaici, and D. Zaninelli, "Assessment of the impact of electric vehicles on the design and effectiveness of electric distribution grid with distributed generation," *Appl. Sci.*, vol. 10, no. 15, p. 5125, Jul. 2020.

[17] J. Coignard, P. MacDougall, F. Stadtmueller, and E. Vrettos, "Will electric vehicles drive distribution grid upgrades?: The case of California," *IEEE Electrific. Mag.*, vol. 7, no. 2, pp. 46–56, Jun. 2019.

[18] D. Steen, L. A. Tuan, O. Carlson, and L. Bertling, "Assessment of electric vehicle charging scenarios based on demographical data," *IEEE Trans. Smart Grid*, vol. 3, no. 3, pp. 1457–1468, Sep. 2012.

[19] R. A. Verzijlbergh, M. O. W. Grond, Z. Lukszo, J. G. Slootweg, and M. D. Ilic, "Network impacts and cost savings of controlled EV charging," *IEEE Trans. Smart Grid*, vol. 3, no. 3, pp. 1203–1212, Sep. 2012.

[20] M. Lillebo, S. Zaferanlouei, A. Zecchino, and H. Farahmand, "Impact of large-scale EV integration and fast chargers in a Norwegian LV grid," *J. Eng.*, vol. 2019, no. 18, pp. 5104–5108, Jul. 2019.

[21] L. Calearo, A. Thingvad, K. Suzuki, and M. Marinelli, "Grid loading due to EV charging profiles based on pseudo-real driving pattern and user behavior," *IEEE Trans. Transport. Electrific.*, vol. 5, no. 3, pp. 683–694, Sep. 2019.

[22] J. Quirós-Tortós, L. F. Ochoa, S. W. Alnaser, and T. Butler, "Control of EV charging points for thermal and voltage management of LV networks," *IEEE Trans. Power Syst.*, vol. 31, no. 4, pp. 3028–3039, Jul. 2016.

[23] A. T. Procopiou, J. Quirós-Tortós, and L. F. Ochoa, "HPC-based probabilistic analysis of LV networks with EVs: Impacts and control," *IEEE Trans. Smart Grid*, vol. 8, no. 3, pp. 1479–1487, May 2017.

[24] C. Crozier, T. Morstyn, and M. McCulloch, "The opportunity for smart charging to mitigate the impact of electric vehicles on transmission and distribution systems," *Appl. Energy*, vol. 268, Jun. 2020, Art. no. 114973.

[25] Synthetic load profiles. *Power Clearing & Settlement Austria (APCS)*. Accessed: Apr. 20, 2021. [Online]. Available: https://www.apcs.at/

[26] Standardlastprofile strom. *Bundesverband Der Energie-Und Wasserwirtschaft (BDEW)*. Accessed: Jul. 13, 2021. [Online]. Available: https://www.bdew.de/

[27] De Vereniging Nederlandse EnergieDataUitwisseling (NEDU). *Verbruiksprofielen-Profielen 2018*. Accessed: Apr. 20, 2021. [Online]. Available: https://www.nedu.nl

[28] NREL. *PVwatts calculator*. Accessed: Apr. 20, 2021. [Online]. Available: https://pvwatts.nrel.gov

[29] S. Wagh, Y. Yu, A. Shekhar, G. R. C. Mouli, and P. Bauer, "Aggregated impact of EV charger type and EV penetration level in improving PV integration in distribution grids," in *Proc. IEEE Transp. Electrific. Conf. Expo (ITEC)*, Jun. 2021, pp. 595–600.

[30] Centraal Bureau voor de Statistiek. *Zonnestroom; Vermogen Bedrijven En Woningen, Regio(Indeling 2018), 2012–2018*. Accessed: Apr. 20, 2021. [Online]. Available: https://opendata.cbs.nl

[31] Rijksdienst voor Ondernemend Nederland (RVO). *Factsheets Zon*. Accessed: Apr. 20, 2021. [Online]. Available: https://www.rvo.nl

[32] Centraal Bureau voor de Statistiek. *Regionale Kerncijfers Nederland*. Accessed: Apr. 20, 2021. [Online]. Available: https://opendata.cbs.nl

[33] G. R. C. Mouli, P. Bauer, and M. Zeman, "System design for a solar powered electric vehicle charging station for workplaces," *Appl. Energy*, vol. 168, pp. 434–443, Apr. 2016.
[34] *Data From Statistik Austria*. Accessed: Apr. 20, 2021. [Online]. Available: https://www.statistik.at/
[35] Centraal Bureau voor de Statistiek (CBS). *Autobezit Naar Regio En Persoonskenmerken, 2018*. Accessed: Apr. 20, 2021. [Online]. Available: https://www.cbs.nl
[36] Y. Yu, A. Shekhar, G. C. R. Mouli, P. Bauer, N. Refa, and R. Bernards, "Impact of uncontrolled charging with mass deployment of electric vehicles on low voltage distribution networks," in *Proc. IEEE Transp. Electrific. Conf. Expo (ITEC)*, Jun. 2020, pp. 766–772.
[37] N. Refa and N. Hubbers, "Impact of smart charging on EVs charging behaviour assessed from real charging events," in *Proc. 32th Int. Electr. Vehicle Symp.*, Lyon, France, 2019. [Online]. Available: https://scholar.google.nl/citations?view_op=view_citation&hl=nl&user=NxZkE04AAAAJ&alert_preview_top_rm=2&citation_for_view=NxZkE04AAAAJ:ufrVoPGSRksC
[38] Rijksdienst voor Ondernemend Nederland (RVO). *Statistics Electric Vehicles and Charging in The Netherlands up to and Including November 2018*. Accessed: Apr. 20, 2021. [Online]. Available: https://www.rvo.nl
[39] Kraftfahrt-Bundesamt (KBA). *Neuzulassungen Nach Umwelt-Merkmalen (fz 14) (New Registrations According to Environmental Characteristics)*. Accessed: Apr. 20, 2021. [Online]. Available: https://www.kba.de
[40] R. Tomschy, M. Herry, G. Sammer, R. Klementschitz, S. Riegler, R. Follmer, D. Gruschwitz, F. Josef, S. Gensasz, R. Kirnbauer, and T. Spiegel, "Österreich unterwegs 2013/2014 (results report for the Austria-wide mobility survey 'Austria on the move 2013/2014),'" Bundesministerium Verkehr, Innovation und Technologie, Vienna, Austria, 2016. [Online]. Available: https://www.bmk.gv.at/themen/verkehrsplanung/statistik/oesterreich_unterwegs.html
[41] T. Schlößer, E. Tröster, and L. Hülsmann, "Probabilistic modeling of charging profiles in low voltage networks," in *Proc. 2nd E-Mobility Power Syst. Integr. Symp.*, Stockholm, Sweden, Oct. 2018, pp. 1–5.
[42] Elaad. *Elaad Open Data Platform, 2018*. Accessed: May 11, 2021. [Online]. Available: https://platform.elaad.io/
[43] *Voltage Disturbances Standard En-50160—Voltage Characteristics in Public Distribution Systems*, Standard EN 50160, 2010.
[44] A. Dubey and S. Santoso, "Electric vehicle charging on residential distribution systems: Impacts and mitigations," *IEEE Access*, vol. 3, pp. 1871–1893, 2015.

YUNHE YU received the M.Sc. degree in sustainable energy technology from the Delft University of Technology, in 2017. She is currently pursuing the Ph.D. degree in electrical engineering. Her research interests include EV integrate in the LV distribution grids and EV smart charging algorithm development.

DAVID REIHS received the B.Sc. degree in physics from the Technical University of Munich, in 2014, and the M.Sc. degree in physical energy and measurement technology from the Technical University of Vienna, in 2018. He is currently working as a Research Engineer with the AIT Austrian Institute of Technology.

SAUMITRA WAGH received the Bachelor of Engineering degree in electrical engineering from Gujarat Technological University, in 2017, and the M.Sc. degree in sustainable energy technology from the Delft University of Technology, in 2020. He is currently working as a Junior Operations Manager Intraday with Northpool B.V.

ADITYA SHEKHAR (Member, IEEE) received the bachelor's degree (Hons.) in electrical from the National Institute of Technology, Surat, India, in 2010, and the M.Sc. *(cum laude)* and Ph.D. degrees in electrical engineering from the Delft University of Technology, Delft, The Netherlands, in June 2015 and January 2020, respectively.

He is currently an Assistant Professor with the DC systems, Energy Conversion and Storage Group, Department of Electrical Sustainable Energy, Delft University of Technology.

DANIEL STAHLEDER received the degree from the Technical University of Munich, in 2020. He is currently working as a Junior Research Engineer with AIT Austrian Institute of Technology.

GAUTHAM RAM CHANDRA MOULI (Member, IEEE) received the bachelor's degree in electrical engineering from the National Institute of Technology Trichy, India, in 2011, and the master's degree in electrical engineering from the Delft University of Technology, in 2013, and the Ph.D. degree from the Delft University, in 2018, for the development of a solar powered V2G electric vehicle charger compatible with CHAdeMO, CCS/COMBO, and designed smart charging algorithms (with PRE Power Developers, ABB, and UT Austin). He is currently an Assistant Professor with the DC systems, Energy Conversion and Storage Group, Department of Electrical Sustainable Energy, Delft University of Technology, The Netherlands. His current research interests include electric vehicles, EV charging, PV systems, power electronics, and demand-side management.

FELIX LEHFUSS was born in Vienna, Austria, in 1982. He received the M.Sc. degree in systems design from the Carinthia University of Applied Sciences, Villach, Austria, in 2010, on the topic of power hardware-in-the-loop simulation. He is currently with the Austrian Institute of Technology (AIT), Vienna, where he is working in the field of electric energy systems. His research interests include mechatronics, electrical systems design, control systems, and simulation technologies

PAVOL BAUER (Senior Member, IEEE) received the master's degree in electrical engineering from the Technical University of Kosice, in 1985, and the Ph.D. degree from the Delft University of Technology, in 1995. He is currently a Full Professor with the Department of Electrical Sustainable Energy, Delft University of Technology, and the Head of the DC Systems, Energy Conversion and Storage Group.